

Dioxidomolybdenum(VI) complex featuring a 2,4-difluoro-substituted amine bis(phenolate) ligand

Christina L. Bowen and Bradley M. Wile*

The School of Science, Technology, and Mathematics, Ohio Northern University, 525 S. Main Street, Ada, OH 45810, USA. *Correspondence e-mail: b-wile@onu.edu

Received 1 April 2021

Accepted 13 May 2021

Edited by S. Parkin, University of Kentucky, USA

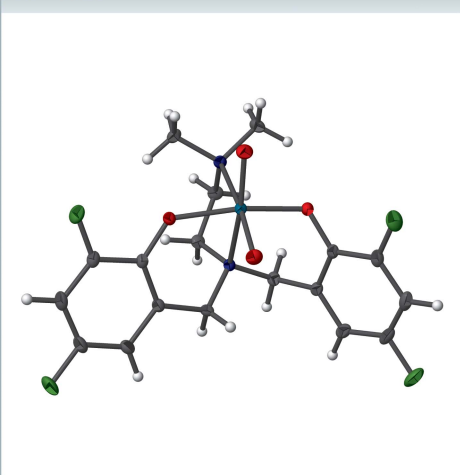
Keywords: crystal structure; molybdenum; oxo; Moco.

CCDC reference: 2083619

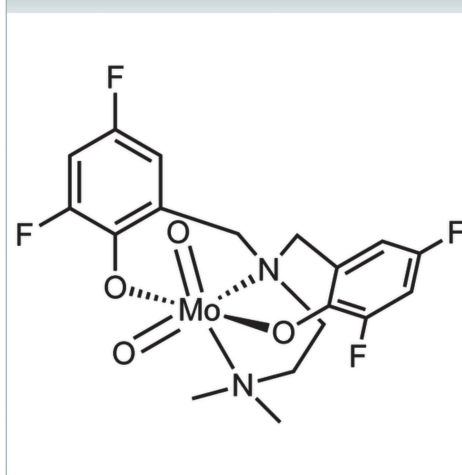
Structural data: full structural data are available from iucrdata.iucr.org

Synthetic complexes containing a *cis*-[MoO₂]²⁺ core are well-established models for the molybdenum co-factor (Moco). Here we report the crystal structure of such a model complex bearing a tetradentate amine bis(phenolate) ligand with fluorine substituents on the phenolate rings, namely, [2,2'-({[2-(dimethylamino)ethyl]azanediyl}bis(methylene))bis(4,6-difluorophenolato)]dioxidomolybdenum(VI), [Mo(C₁₈H₁₈F₄N₂O₂)O₂]. Distortion from idealized octahedral symmetry about the Mo center is evident in the large O=Mo=O angle [108.54 (4)°] and the small N–Mo–O_{phenolate} angles [79.79 (4), 81.21 (3), 77.83 (3), and 84.59 (3)°]. The dihedral angle between the phenolate rings is 60.06 (4)°, and π - π stacking is observed between aromatic rings related by inversion (1 - x, 1 - y, 1 - z). The lower data-collection temperature of 150 K vs room-temperature data collection reported previously [KOWXIF; Cao *et al.* (2014). *Transit. Met. Chem.* **39**, 933–937] and larger 2θ range for data collection (5.8–66.6° versus 6–54.96°) led to a structure with lower R_1 and ωR_2 values (0.019 and 0.049 vs 0.0310 and 0.0566 for KOWXIF). Comparison of the metrical parameters with KOWXIF suggests that this dataset offers a more realistic depiction of bonding within the Mo^{VI}=O moiety.

3D view



Chemical scheme



Structure description

Molybdenum-containing metalloenzymes are abundant and serve as excellent motivation for biomimetic catalyst development. The relevance of xanthine oxidase, DMSO reductase, sulfite oxidase to oxygen atom transfer and proton-coupled electron-transfer reactions have driven interest in related mononuclear Mo complexes for generating H₂ or expanding opportunities for storage of energy generated by increasingly efficient solar cells. The native enzymes contain a molybdenum cofactor (Moco) in which the Mo^{VI}=O moiety is supported by dithiolene-containing molybdopterin ligands (Kisker *et al.*, 1997).

Table 1

Comparison of lengths and angles between this work and previous report.

	This work (CLB-1-87)	KOWXIF (Cao <i>et al.</i> , 2014)	
Mo—O1	1.9788 (8)	1.976 (3)	
Mo—O2	1.9287 (8)	1.919 (3)	
Mo—O3	1.7062 (8)	1.693 (2)	difference greater than ± 3 s.u.
Mo—O4	1.7123 (7)	1.700 (3)	difference greater than ± 3 s.u.
Mo—N1	2.4008 (8)	2.395 (3)	
Mo—N2	2.4117 (9)	2.412 (3)	
O1—Mo1—O3	98.19 (4)	98.6 (1)	
O1—Mo1—O4	93.41 (4)	93.4 (1)	
O1—Mo1—N1	79.79 (3)	79.7 (1)	
O1—Mo1—N2	84.59 (3)	84.5 (1)	
O2—Mo1—O3	99.96 (4)	99.9 (1)	
O2—Mo1—O4	95.43 (4)	95.8 (1)	
O2—Mo1—N1	77.83 (3)	77.5 (1)	
O2—Mo1—N2	81.21 (3)	81.0 (1)	
O3—Mo1—O4	108.54 (4)	108.2 (1)	
N1—Mo1—N2	73.84 (3)	73.8 (1)	
N1—C1—C2—N2	-55.84 (11)	56.4 (4)	

A robust molybdenum–oxo complex bearing a pentadentate pyridyl ligand was notably shown to catalytically generate H₂ from water at a low overpotential (Karunadasa *et al.*, 2010). Related molybdenum–oxo complexes featuring an amine bis(phenolate) moiety have been similarly shown to promote H₂ generation (Cao *et al.*, 2014) and oxygen atom transfer (Maurya *et al.*, 2016). Insight into the structural features that enable such activity at the Mo=O moiety are thus an important component of iterating the design of these species for use as sustainable aqueous catalysts.

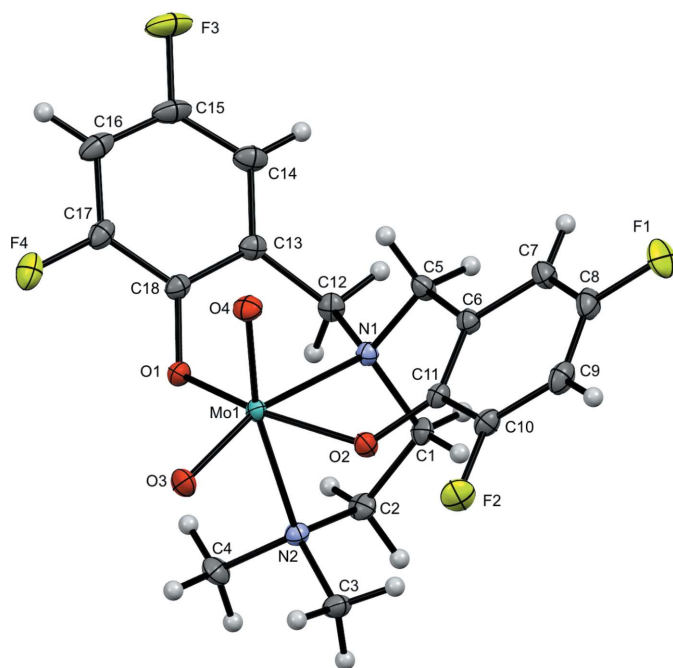


Figure 1

Molecular structure of **2** with 50% displacement ellipsoids and the numbering scheme for non-H atoms.

The Mo complex reported here (**2**, Fig. 1) is chemically identical to that reported by Cao *et al.* (2014, KOWXIF). The lower collection temperature (150 K *versus* room temperature in KOWXIF) and larger 2θ range for data collection (5.8–66.6° *versus* 6–54.96° in the previous report) led to a structure solution with lower R_1 and ωR_2 values (0.019 and 0.049 *versus* 0.0310 and 0.0566 in KOWXIF). Slight differences in the bond lengths for the compound in these structures warrant further comment and may be of interest from a mechanistic perspective. For example, it is generally accepted that an Mo=O bond in the *cis*-[MoO₂]²⁺ core of DMSO reductase model compounds is formally strengthened (consistent with Mo≡O) during oxygen atom transfer (Enemark, *et al.*, 2004).

Both structures have $P\bar{1}$ space-group symmetry, though a , c , β , and γ were different by ± 3 s.u. While the Mo–O(phenolate) and Mo–N bonds in this structure are nearly identical to those reported by Cao *et al.*, the Mo=O bond lengths reported here are notably longer than those in KOWXIF and are in line with expectations for related Mo^{VI}–oxo species (Enemark, *et al.*, 2004). However, these differences in bond length are within the accuracy limits for light atoms imposed by the spherical atom scattering factor approximation (*e.g.* Dawson, 1964). Relevant lengths and angles for both are summarized in Table 1. Differences in the metrical parameters for these structures suggest that the model presented here gives a better representation of the bonding for **2**, when compared with other Mo^{VI} oxo species.

No hydrogen bonding was observed, though short contacts exist between inversion-related molecules contained in the unit cell. The orientation of one phenolate ring brings the *ortho* carbons C16 and C18ⁱ [symmetry code: (i) $1 - x, 1 - y, 1 - z$] in close proximity [3.2807 (15) Å, *i.e.* ~ 0.12 Å closer than the sum of the vdW radii]. Close contact is noted for the *para* F3 and proximal *meta* C16ⁱⁱ [symmetry code: (ii) $2 - x, 2 - y, 1 - z$] of an adjacent inversion-related molecule [3.1622 (14) Å, *i.e.* ~ 0.01 Å closer than the sum of the vdW radii]. This marginally short contact is consistent with π – π

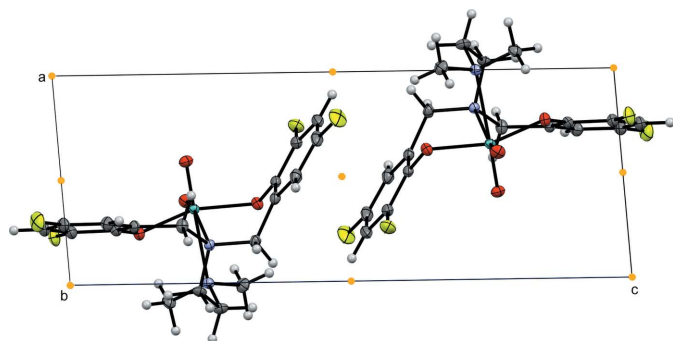


Figure 2
Packing plot (viewed along *b*) showing π - π stacking of fluorinated (F3, F4) phenolate rings related by inversion. Orange dots represent centers of inversion.

stacking between the phenolate rings related by the inversion center; this interaction is shown in Fig. 2. A similar, though much more pronounced contact is noted between *ortho* F2 and the amine methyl group, C3ⁱⁱⁱ [symmetry code: (iii) $-x, -y, -z$] [2.9229 (13) Å, ~ 0.247 Å closer than the sum of the vdW radii]. Each Mo^{VI}=O moiety lies above planes defined by the amine bis(phenolate) ligand and the other oxo [0.3037 (4) Å above the plane defined by O1, O2, O4, and N2; 0.2696 (4) Å above the plane defined by O1, O2, O3, and N1]. This distortion from an ideal octahedral geometry is consistent with related Mo^{VI} oxo species, and is evident in the large O3–Mo1–O4 bond angle [108.54 (4)°]. The dihedral between aromatic rings was found to be 60.06 (4)°. The torsion angle along the diamine N1–C1–C2–N2 [–55.84 (11)°] is consistent with the *syn* conformation of amine donors within the unstrained five-membered ring formed upon chelation.

Synthesis and crystallization

The ligand H₂ONNO^F (**1**) was prepared by the method reported previously (Graziano *et al.*, 2019). The Mo complex (**2**) was prepared using a modified version of the method reported by Lehtonen & Sillanpää (2005). The reaction scheme is shown in Fig. 3. MoO₂(*acac*)₂ (0.330 g, 1.01 mmol) and the ligand H₂ONNO^F (**1**; 0.373 g, 1.00 mmol) were combined in a 20 ml scintillation vial with a PTFE-coated stir bar and suspended in 10 ml of anhydrous methanol. The reaction mixture was left to stir for 4 h at 295 K, at which time solvent and other volatiles were removed *in vacuo* to yield a yellow solid (0.500 g, 1.00 mmol, >99%). The product was purified by column chromatography on silica using an increasing linear gradient of dichloromethane in acetone as

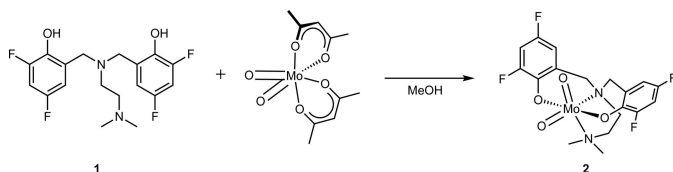


Figure 3
Reaction scheme.

Table 2
Experimental details.

Crystal data	[Mo(C ₁₈ H ₁₈ F ₄ N ₂ O ₂)O ₂]
Chemical formula	498.28
<i>M_r</i>	Triclinic, <i>P</i> $\bar{1}$
Crystal system, space group	150
Temperature (K)	7.3179 (4), 8.0093 (4), 17.5057 (9)
<i>a</i> , <i>b</i> , <i>c</i> (Å)	91.8513 (18), 92.9102 (18), 116.6842 (16)
α , β , γ (°)	913.82 (8)
<i>V</i> (Å ³)	2
<i>Z</i>	Mo <i>K</i> α
Radiation type	0.79
μ (mm ⁻¹)	Crystal size (mm)
Crystal size (mm)	0.26 × 0.24 × 0.15
Data collection	
Diffractometer	Bruker AXS D8 Quest CMOS diffractometer
Absorption correction	Multi-scan (<i>SADABS</i> ; Krause <i>et al.</i> , 2015)
<i>T</i> _{min} , <i>T</i> _{max}	0.702, 0.747
No. of measured, independent and observed [<i>I</i> > 2 σ (<i>I</i>)] reflections	47859, 7013, 6541
<i>R</i> _{int}	0.027
(<i>sin</i> θ / λ) _{max} (Å ⁻¹)	0.772
Refinement	
<i>R</i> [<i>F</i> ² > 2 σ (<i>F</i> ²)], <i>wR</i> (<i>F</i> ²), <i>S</i>	0.019, 0.049, 1.12
No. of reflections	7013
No. of parameters	266
H-atom treatment	H-atom parameters constrained
$\Delta\rho$ _{max} , $\Delta\rho$ _{min} (e Å ⁻³)	0.92, –0.48

Computer programs: *APEX3* and *SAINT* (Bruker, 2018), *SHELXT* (Sheldrick, 2015a), *SHELXL2018/3* (Sheldrick, 2015b), *ShelXle* (Hübschle *et al.*, 2011) and *Mercury* (Macrae *et al.*, 2020).

the eluent. After removing the solvent and other volatiles, single crystals suitable for diffraction studies were obtained by slow evaporation from a concentrated solution of acetone. Characterization data for this compound match those previously reported by Cao *et al.* (2014). M.p. = 463–467 K.

Refinement

Crystal data, data collection and structure refinement details are summarized in Table 2. No disorder or solvent were present.

Acknowledgements

Data collection and refinement were conducted by Matthias Zeller (Purdue University). The authors wish to thank Brendan Graziano for helpful discussions.

Funding information

This material is based upon work supported by the National Science Foundation through the Major Research Instrumentation Program under grant No. CHE 1625543 (funding for the single-crystal X-ray diffractometer). Acknowledgment is made to the donors of The American Chemical Society Petroleum Research Fund for support of this research (grant No. 56549-UR3). Partial funding for this project was provided

by the Getty College of Arts and Sciences at Ohio Northern University.

References

- Bruker (2018). *APEX3* and *SAINT*. Bruker AXS Inc. Madison, Wisconsin, USA.
- Cao, J.-P., Zhao, J.-X., Lu, H.-X. & Zhan, S.-Z. (2014). *Transition Met. Chem.* **39**, 933–937.
- Dawson, B. (1964). *Acta Cryst.* **17**, 990–996.
- Enemark, J. H., Cooney, J. J. A., Wang, J.-J. & Holm, R. H. (2004). *Chem. Rev.* **104**, 1175–1200.
- Graziano, B. J., Collins, E. M., McCutcheon, N. C., Griffith, C. L., Braunscheidel, N. M., Perrine, T. M. & Wile, B. M. (2019). *Inorg. Chim. Acta*, **484**, 185–196.
- Hübschle, C. B., Sheldrick, G. M. & Dittrich, B. (2011). *J. Appl. Cryst.* **44**, 1281–1284.
- Karunadasa, H. I., Chang, C. J. & Long, J. R. (2010). *Nature*, **464**, 1329–1333.
- Kisker, C., Schindelin, H. & Rees, D. C. (1997). *Annu. Rev. Biochem.* **66**, 233–267.
- Krause, L., Herbst-Irmer, R., Sheldrick, G. M. & Stalke, D. (2015). *J. Appl. Cryst.* **48**, 3–10.
- Lehtonen, A. & Sillanpää, R. (2005). *Polyhedron*, **24**, 257–265.
- Macrae, C. F., Sovago, I., Cottrell, S. J., Galek, P. T. A., McCabe, P., Pidcock, E., Platings, M., Shields, G. P., Stevens, J. S., Towler, M. & Wood, P. A. (2020). *J. Appl. Cryst.* **53**, 226–235.
- Maurya, M. R., Uprety, B. & Avecilla, F. (2016). *Eur. J. Inorg. Chem.* pp. 4802–4813.
- Sheldrick, G. M. (2015a). *Acta Cryst.* **A71**, 3–8.
- Sheldrick, G. M. (2015b). *Acta Cryst.* **C71**, 3–8.

full crystallographic data

IUCrData (2021). 6, x210516 [https://doi.org/10.1107/S2414314621005162]

Dioxidomolybdenum(VI) complex featuring a 2,4-difluoro-substituted amine bis(phenolate) ligand

Christina L. Bowen and Bradley M. Wile

[2,2'-([2-(Dimethylamino)ethyl]azanediy)bis(methylene))bis(4,6-difluorophenolato)]dioxidomolybdenum(VI),

Crystal data

[Mo(C₁₈H₁₈F₄N₂O₂)O₂]

$M_r = 498.28$

Triclinic, *P*1

$a = 7.3179$ (4) Å

$b = 8.0093$ (4) Å

$c = 17.5057$ (9) Å

$\alpha = 91.8513$ (18)°

$\beta = 92.9102$ (18)°

$\gamma = 116.6842$ (16)°

$V = 913.82$ (8) Å³

$Z = 2$

$F(000) = 500$

$D_x = 1.811$ Mg m⁻³

Mo *K* α radiation, $\lambda = 0.71073$ Å

Cell parameters from 9173 reflections

$\theta = 2.3$ – 33.2 °

$\mu = 0.79$ mm⁻¹

$T = 150$ K

Block, orange

$0.26 \times 0.24 \times 0.15$ mm

Data collection

Bruker AXS D8 Quest CMOS
diffractometer

Radiation source: fine focus sealed tube X-ray
source

Triumph curved graphite crystal
monochromator

Detector resolution: 10.4167 pixels mm⁻¹

ω and ϕ scans

Absorption correction: multi-scan
(*SADABS*; Krause *et al.*, 2015)

$T_{\min} = 0.702$, $T_{\max} = 0.747$

47859 measured reflections

7013 independent reflections

6541 reflections with $I > 2\sigma(I)$

$R_{\text{int}} = 0.027$

$\theta_{\max} = 33.3$ °, $\theta_{\min} = 2.9$ °

$h = -11 \rightarrow 11$

$k = -12 \rightarrow 12$

$l = -26 \rightarrow 25$

Refinement

Refinement on F^2

Least-squares matrix: full

$R[F^2 > 2\sigma(F^2)] = 0.019$

$wR(F^2) = 0.049$

$S = 1.12$

7013 reflections

266 parameters

0 restraints

Primary atom site location: structure-invariant
direct methods

Secondary atom site location: difference Fourier
map

Hydrogen site location: inferred from
neighbouring sites

H-atom parameters constrained

$w = 1/[\sigma^2(F_o^2) + (0.0194P)^2 + 0.4598P]$

where $P = (F_o^2 + 2F_c^2)/3$

$(\Delta/\sigma)_{\max} = 0.001$

$\Delta\rho_{\max} = 0.92$ e Å⁻³

$\Delta\rho_{\min} = -0.48$ e Å⁻³

Extinction correction: *SHELXL2018/3*
(Sheldrick 2015b),

$F_c^* = kF_c[1 + 0.001x F_c^2 \lambda^3 / \sin(2\theta)]^{-1/4}$

Extinction coefficient: 0.0171 (8)

Special details

Geometry. All esds (except the esd in the dihedral angle between two l.s. planes) are estimated using the full covariance matrix. The cell esds are taken into account individually in the estimation of esds in distances, angles and torsion angles; correlations between esds in cell parameters are only used when they are defined by crystal symmetry. An approximate (isotropic) treatment of cell esds is used for estimating esds involving l.s. planes.

Fractional atomic coordinates and isotropic or equivalent isotropic displacement parameters (\AA^2)

	<i>x</i>	<i>y</i>	<i>z</i>	$U_{\text{iso}}^*/U_{\text{eq}}$
Mo1	0.35403 (2)	0.27852 (2)	0.23176 (2)	0.01088 (3)
F1	0.30483 (14)	0.85179 (12)	−0.04843 (5)	0.03105 (18)
F2	0.23146 (13)	0.24459 (11)	−0.02051 (4)	0.02510 (15)
F3	0.77983 (14)	0.98402 (12)	0.50141 (5)	0.0357 (2)
F4	0.74459 (12)	0.40003 (12)	0.42642 (5)	0.02571 (15)
O2	0.24235 (12)	0.28426 (11)	0.13025 (4)	0.01475 (13)
O1	0.37637 (12)	0.30006 (11)	0.34515 (4)	0.01499 (13)
O3	0.39279 (13)	0.08489 (11)	0.21952 (5)	0.01831 (15)
O4	0.58252 (12)	0.47327 (11)	0.22506 (5)	0.01743 (14)
N1	0.18199 (13)	0.46786 (12)	0.25408 (5)	0.01204 (14)
N2	0.00004 (13)	0.06353 (12)	0.24545 (5)	0.01375 (15)
C1	−0.03936 (15)	0.35240 (15)	0.22876 (6)	0.01565 (18)
H1A	−0.055488	0.333606	0.172183	0.019*
H1B	−0.118429	0.419086	0.244487	0.019*
C2	−0.12266 (16)	0.16343 (15)	0.26393 (7)	0.01739 (18)
H2A	−0.119764	0.181957	0.320249	0.021*
H2B	−0.267036	0.086095	0.244251	0.021*
C3	−0.08879 (17)	−0.05342 (15)	0.17262 (6)	0.01864 (19)
H3A	−0.099801	0.024782	0.132488	0.028*
H3B	−0.225312	−0.153590	0.180273	0.028*
H3C	0.000294	−0.108430	0.157166	0.028*
C4	−0.01342 (18)	−0.06387 (16)	0.30686 (7)	0.0197 (2)
H4A	−0.157319	−0.152867	0.311224	0.029*
H4B	0.043768	0.009500	0.355647	0.029*
H4C	0.064405	−0.132458	0.294289	0.029*
C5	0.27534 (17)	0.63562 (14)	0.20820 (6)	0.01565 (18)
H5A	0.419181	0.712021	0.228692	0.019*
H5B	0.201603	0.711773	0.216119	0.019*
C6	0.27467 (16)	0.59822 (14)	0.12285 (6)	0.01432 (17)
C7	0.29093 (17)	0.74157 (16)	0.07532 (6)	0.01792 (19)
H7	0.303492	0.856995	0.096826	0.021*
C8	0.28844 (18)	0.71284 (17)	−0.00284 (7)	0.0202 (2)
C9	0.26776 (18)	0.54719 (17)	−0.03773 (6)	0.0203 (2)
H9	0.265023	0.529975	−0.091799	0.024*
C10	0.25135 (17)	0.40861 (16)	0.01002 (6)	0.01692 (18)
C11	0.25771 (15)	0.43022 (14)	0.08992 (6)	0.01363 (16)
C12	0.19506 (17)	0.53698 (15)	0.33577 (6)	0.01572 (18)
H12A	0.159066	0.642284	0.336701	0.019*
H12B	0.091704	0.435217	0.363450	0.019*

C13	0.40118 (16)	0.60117 (15)	0.37784 (6)	0.01528 (17)
C14	0.50261 (19)	0.77546 (16)	0.41804 (6)	0.0204 (2)
H14	0.449901	0.864217	0.415639	0.024*
C15	0.6818 (2)	0.81511 (17)	0.46142 (7)	0.0238 (2)
C16	0.76763 (18)	0.69352 (18)	0.46549 (7)	0.0229 (2)
H16	0.892175	0.725565	0.495342	0.028*
C17	0.66479 (17)	0.52275 (16)	0.42429 (6)	0.01820 (19)
C18	0.47924 (16)	0.47139 (14)	0.38146 (6)	0.01454 (17)

Atomic displacement parameters (\AA^2)

	U^{11}	U^{22}	U^{33}	U^{12}	U^{13}	U^{23}
Mo1	0.01022 (4)	0.01143 (4)	0.01228 (4)	0.00609 (3)	0.00069 (3)	0.00012 (3)
F1	0.0408 (5)	0.0298 (4)	0.0230 (4)	0.0155 (4)	0.0016 (3)	0.0148 (3)
F2	0.0352 (4)	0.0255 (4)	0.0153 (3)	0.0151 (3)	-0.0014 (3)	-0.0060 (3)
F3	0.0359 (5)	0.0233 (4)	0.0305 (4)	-0.0005 (3)	-0.0042 (3)	-0.0120 (3)
F4	0.0204 (3)	0.0338 (4)	0.0257 (4)	0.0149 (3)	-0.0020 (3)	0.0034 (3)
O2	0.0190 (3)	0.0142 (3)	0.0122 (3)	0.0086 (3)	0.0002 (3)	0.0003 (2)
O1	0.0168 (3)	0.0141 (3)	0.0131 (3)	0.0064 (3)	-0.0015 (3)	0.0004 (2)
O3	0.0197 (4)	0.0168 (3)	0.0226 (4)	0.0121 (3)	0.0000 (3)	-0.0005 (3)
O4	0.0132 (3)	0.0168 (3)	0.0207 (4)	0.0052 (3)	0.0030 (3)	0.0011 (3)
N1	0.0128 (3)	0.0130 (3)	0.0117 (3)	0.0070 (3)	0.0008 (3)	0.0003 (3)
N2	0.0130 (4)	0.0134 (4)	0.0146 (4)	0.0056 (3)	0.0011 (3)	0.0011 (3)
C1	0.0116 (4)	0.0176 (4)	0.0199 (5)	0.0088 (3)	-0.0005 (3)	0.0006 (3)
C2	0.0114 (4)	0.0181 (4)	0.0228 (5)	0.0066 (3)	0.0032 (3)	0.0013 (4)
C3	0.0171 (4)	0.0155 (4)	0.0183 (5)	0.0035 (4)	-0.0019 (4)	-0.0024 (4)
C4	0.0220 (5)	0.0165 (4)	0.0196 (5)	0.0073 (4)	0.0040 (4)	0.0067 (4)
C5	0.0218 (5)	0.0123 (4)	0.0142 (4)	0.0088 (4)	0.0018 (3)	0.0012 (3)
C6	0.0147 (4)	0.0148 (4)	0.0136 (4)	0.0067 (3)	0.0007 (3)	0.0019 (3)
C7	0.0195 (5)	0.0169 (4)	0.0180 (5)	0.0086 (4)	0.0009 (4)	0.0047 (4)
C8	0.0194 (5)	0.0226 (5)	0.0178 (5)	0.0084 (4)	0.0009 (4)	0.0086 (4)
C9	0.0187 (5)	0.0276 (5)	0.0132 (4)	0.0092 (4)	0.0004 (4)	0.0041 (4)
C10	0.0165 (4)	0.0203 (5)	0.0133 (4)	0.0080 (4)	-0.0004 (3)	-0.0012 (3)
C11	0.0130 (4)	0.0159 (4)	0.0119 (4)	0.0065 (3)	0.0002 (3)	0.0009 (3)
C12	0.0183 (4)	0.0188 (4)	0.0129 (4)	0.0108 (4)	0.0025 (3)	-0.0004 (3)
C13	0.0177 (4)	0.0154 (4)	0.0111 (4)	0.0060 (3)	0.0020 (3)	0.0001 (3)
C14	0.0250 (5)	0.0170 (5)	0.0155 (5)	0.0062 (4)	0.0032 (4)	-0.0019 (4)
C15	0.0247 (5)	0.0192 (5)	0.0152 (5)	-0.0006 (4)	0.0014 (4)	-0.0041 (4)
C16	0.0177 (5)	0.0267 (5)	0.0138 (5)	0.0008 (4)	-0.0008 (4)	0.0007 (4)
C17	0.0149 (4)	0.0230 (5)	0.0137 (4)	0.0059 (4)	0.0006 (3)	0.0030 (4)
C18	0.0146 (4)	0.0158 (4)	0.0107 (4)	0.0046 (3)	0.0007 (3)	0.0011 (3)

Geometric parameters (\AA , $^\circ$)

Mo1—O3	1.7062 (8)	C4—H4A	0.9800
Mo1—O4	1.7123 (8)	C4—H4B	0.9800
Mo1—O2	1.9287 (8)	C4—H4C	0.9800
Mo1—O1	1.9788 (8)	C5—C6	1.5137 (15)

Mo1—N1	2.4008 (8)	C5—H5A	0.9900
Mo1—N2	2.4117 (9)	C5—H5B	0.9900
F1—C8	1.3554 (13)	C6—C11	1.3968 (14)
F2—C10	1.3444 (13)	C6—C7	1.4048 (15)
F3—C15	1.3605 (14)	C7—C8	1.3779 (16)
F4—C17	1.3506 (14)	C7—H7	0.9500
O2—C11	1.3494 (12)	C8—C9	1.3835 (18)
O1—C18	1.3494 (12)	C9—C10	1.3767 (16)
N1—C5	1.4894 (13)	C9—H9	0.9500
N1—C1	1.4936 (13)	C10—C11	1.3997 (14)
N1—C12	1.4994 (13)	C12—C13	1.4993 (15)
N2—C4	1.4825 (14)	C12—H12A	0.9900
N2—C2	1.4863 (14)	C12—H12B	0.9900
N2—C3	1.4890 (14)	C13—C18	1.3945 (15)
C1—C2	1.5202 (15)	C13—C14	1.3956 (15)
C1—H1A	0.9900	C14—C15	1.3809 (18)
C1—H1B	0.9900	C14—H14	0.9500
C2—H2A	0.9900	C15—C16	1.377 (2)
C2—H2B	0.9900	C16—C17	1.3835 (16)
C3—H3A	0.9800	C16—H16	0.9500
C3—H3B	0.9800	C17—C18	1.3965 (15)
C3—H3C	0.9800		
O3—Mo1—O4	108.54 (4)	H4A—C4—H4C	109.5
O3—Mo1—O2	99.96 (4)	H4B—C4—H4C	109.5
O4—Mo1—O2	95.43 (4)	N1—C5—C6	116.27 (8)
O3—Mo1—O1	98.19 (4)	N1—C5—H5A	108.2
O4—Mo1—O1	93.41 (4)	C6—C5—H5A	108.2
O2—Mo1—O1	156.09 (3)	N1—C5—H5B	108.2
O3—Mo1—N1	160.10 (4)	C6—C5—H5B	108.2
O4—Mo1—N1	91.35 (3)	H5A—C5—H5B	107.4
O2—Mo1—N1	77.83 (3)	C11—C6—C7	119.31 (10)
O1—Mo1—N1	79.79 (3)	C11—C6—C5	123.44 (9)
O3—Mo1—N2	86.27 (4)	C7—C6—C5	117.24 (9)
O4—Mo1—N2	165.19 (3)	C8—C7—C6	119.25 (10)
O2—Mo1—N2	81.21 (3)	C8—C7—H7	120.4
O1—Mo1—N2	84.59 (3)	C6—C7—H7	120.4
N1—Mo1—N2	73.84 (3)	F1—C8—C7	119.02 (11)
C11—O2—Mo1	130.56 (7)	F1—C8—C9	117.80 (11)
C18—O1—Mo1	118.88 (6)	C7—C8—C9	123.17 (10)
C5—N1—C1	110.73 (8)	C10—C9—C8	116.50 (10)
C5—N1—C12	107.20 (8)	C10—C9—H9	121.7
C1—N1—C12	107.89 (8)	C8—C9—H9	121.7
C5—N1—Mo1	108.18 (6)	F2—C10—C9	119.27 (10)
C1—N1—Mo1	107.55 (6)	F2—C10—C11	117.50 (10)
C12—N1—Mo1	115.29 (6)	C9—C10—C11	123.23 (10)
C4—N2—C2	109.15 (9)	O2—C11—C6	124.11 (9)
C4—N2—C3	107.68 (9)	O2—C11—C10	117.37 (9)

C2—N2—C3	109.18 (8)	C6—C11—C10	118.50 (9)
C4—N2—Mo1	109.89 (6)	C13—C12—N1	114.57 (8)
C2—N2—Mo1	111.74 (6)	C13—C12—H12A	108.6
C3—N2—Mo1	109.11 (6)	N1—C12—H12A	108.6
N1—C1—C2	110.46 (8)	C13—C12—H12B	108.6
N1—C1—H1A	109.6	N1—C12—H12B	108.6
C2—C1—H1A	109.6	H12A—C12—H12B	107.6
N1—C1—H1B	109.6	C18—C13—C14	120.78 (10)
C2—C1—H1B	109.6	C18—C13—C12	116.82 (9)
H1A—C1—H1B	108.1	C14—C13—C12	122.11 (10)
N2—C2—C1	111.22 (9)	C15—C14—C13	118.05 (11)
N2—C2—H2A	109.4	C15—C14—H14	121.0
C1—C2—H2A	109.4	C13—C14—H14	121.0
N2—C2—H2B	109.4	F3—C15—C16	118.40 (11)
C1—C2—H2B	109.4	F3—C15—C14	118.20 (12)
H2A—C2—H2B	108.0	C16—C15—C14	123.39 (11)
N2—C3—H3A	109.5	C15—C16—C17	117.20 (11)
N2—C3—H3B	109.5	C15—C16—H16	121.4
H3A—C3—H3B	109.5	C17—C16—H16	121.4
N2—C3—H3C	109.5	F4—C17—C16	119.01 (10)
H3A—C3—H3C	109.5	F4—C17—C18	118.73 (10)
H3B—C3—H3C	109.5	C16—C17—C18	122.26 (11)
N2—C4—H4A	109.5	O1—C18—C13	120.64 (9)
N2—C4—H4B	109.5	O1—C18—C17	121.10 (10)
H4A—C4—H4B	109.5	C13—C18—C17	118.26 (10)
N2—C4—H4C	109.5		
C5—N1—C1—C2	168.55 (8)	C9—C10—C11—O2	-179.23 (10)
C12—N1—C1—C2	-74.42 (10)	F2—C10—C11—C6	-178.89 (9)
Mo1—N1—C1—C2	50.54 (9)	C9—C10—C11—C6	2.21 (16)
C4—N2—C2—C1	152.57 (9)	C5—N1—C12—C13	-79.49 (11)
C3—N2—C2—C1	-89.97 (10)	C1—N1—C12—C13	161.21 (9)
Mo1—N2—C2—C1	30.82 (10)	Mo1—N1—C12—C13	41.02 (11)
N1—C1—C2—N2	-55.84 (11)	N1—C12—C13—C18	-57.38 (13)
C1—N1—C5—C6	-61.33 (11)	N1—C12—C13—C14	128.74 (11)
C12—N1—C5—C6	-178.78 (9)	C18—C13—C14—C15	-0.08 (16)
Mo1—N1—C5—C6	56.29 (10)	C12—C13—C14—C15	173.57 (10)
N1—C5—C6—C11	-21.87 (15)	C13—C14—C15—F3	-179.23 (10)
N1—C5—C6—C7	157.75 (9)	C13—C14—C15—C16	1.60 (18)
C11—C6—C7—C8	0.42 (16)	F3—C15—C16—C17	179.98 (11)
C5—C6—C7—C8	-179.21 (10)	C14—C15—C16—C17	-0.85 (18)
C6—C7—C8—F1	-179.79 (10)	C15—C16—C17—F4	179.60 (10)
C6—C7—C8—C9	0.90 (18)	C15—C16—C17—C18	-1.46 (17)
F1—C8—C9—C10	-179.97 (10)	Mo1—O1—C18—C13	68.58 (11)
C7—C8—C9—C10	-0.66 (17)	Mo1—O1—C18—C17	-112.20 (9)
C8—C9—C10—F2	-179.82 (10)	C14—C13—C18—O1	177.19 (10)
C8—C9—C10—C11	-0.93 (17)	C12—C13—C18—O1	3.22 (14)
Mo1—O2—C11—C6	-31.59 (15)	C14—C13—C18—C17	-2.06 (16)

Mo1—O2—C11—C10	149.93 (8)	C12—C13—C18—C17	-176.03 (9)
C7—C6—C11—O2	179.65 (10)	F4—C17—C18—O1	2.58 (15)
C5—C6—C11—O2	-0.74 (16)	C16—C17—C18—O1	-176.36 (10)
C7—C6—C11—C10	-1.89 (15)	F4—C17—C18—C13	-178.18 (9)
C5—C6—C11—C10	177.72 (10)	C16—C17—C18—C13	2.88 (16)
F2—C10—C11—O2	-0.32 (14)		
